IEEE Access
Multidisciplinary | Rapid Review | Open Access Journal

Received 7 October 2023, accepted 25 October 2023, date of publication 27 October 2023, date of current version 8 November 2023.

Digital Object Identifier 10.1109/ACCESS.2023.3328214

RESEARCH ARTICLE

Distributed Subcarrier Assignment and Discrete Power Allocation for Multi-UAV Millimeter-Wave Cooperative OFDMA Networks With Heterogeneous QoS Consideration

TONG WANG[1,2], (Member, IEEE), CHUANCHUAN YOU[1,3], (Member, IEEE), ZHOU HE[1,2], AND YOUTIAN WANG[4]

[1]School of Information Engineering, Hubei University of Economics, Wuhan, Hubei 430205, China
[2]Hubei Internet Finance Information Engineering Technology Research Center, Hubei University of Economics, Wuhan, Hubei 430205, China
[3]School of Computer Science, Wuhan University, Wuhan 430072, China
[4]School of Information Management, Hubei University of Economics, Wuhan, Hubei 430205, China

Corresponding author: Chuanchuan You (extremfly@gmail.com)

This work was supported in part by the General Program of Natural Science Foundation of Hubei Province of China under Grant 2022CFB076, in part by the Artificial Intelligence Innovation Project of Wuhan Science and Technology Bureau under Grant 2022010702040068, and in part by the Key Projects of Science and Technology Research Plan of Hubei Provincial Department of Education under Grant D20202203.

ABSTRACT In this paper, we formulate Subcarrier Assignment and Discrete Power Allocation for multi-UAV millimeter-wave cooperative Orthogonal Frequency Division Multiple Access (OFDMA) networks as a joint optimization problem considering the heterogeneous user data rate quality-of-service (QoS) requirements. The formulated joint optimization problem, named Discrete Power and Subcarrier Allocation (DPSA), is a nonconvex and mixed-integer nonlinear programming (MINP) problem, making it NP-hard to solve. We then transform the DPSA into the Subcarrier and Power Resource Efficient Cooperative Potential Game (SRECPG) based on game theory which facilitates distributed execution. We analyze the conditions under which a Nash Equilibrium (NE) exists in the SRECPG and provide rigorous proof of its existence. Furthermore, to enhance computational efficiency, we propose a BR-SSO algorithm based on better response dynamics. BR-SSO dramatically reduces the computational burden compared to the best response dynamics based on local exhaustive search (BRLES) while still ensuring convergence to a NE. Through extensive simulations, we demonstrated the effectiveness of the proposed SRECPG and BR-SSO algorithms. The results show significant improvements in throughput, fairness, and QoS guarantees compared to the baseline schemes. Our approach offers valuable insights into the design of efficient resource allocation schemes for multi-UAV millimeter-wave networks with varying QoS demands.

INDEX TERMS Constrained potential game, downlink multi-cell OFDMA, nash equilibrium, unmanned aerial vehicle, blockage, millimeter-wave, resource allocation.

I. INTRODUCTION

In recent years, Unmanned Aerial Vehicles (UAVs) have emerged as a promising solution for providing communication services in various scenarios. With their ability to operate in remote or inaccessible areas, UAVs offer a flexible and rapidly deployable platform that can support a wide range of applications, including disaster response, surveillance, and wireless communication coverage in underserved regions [1], [2].

Orthogonal Frequency Division Multiple Access (OFDMA), a key component of the Long-Term Evolution (LTE), fifth-generation (5G) and 5G beyond cellular networks, has garnered significant attention because of its

The associate editor coordinating the review of this manuscript and approving it for publication was Yunlong Cai.

ability to efficiently allocate subcarriers to multiple users, thus enabling high data rates and spectral efficiency [3]. Moreover, the utilization of millimeter-wave (mmWave) frequencies allows for a substantial increase in available bandwidth, offering the potential to support ultra-high data rates in wireless communication systems. The combination of OFDMA and mmWave technologies has become a phenomenon in the field of wireless communication, providing a promising approach to overcome the limitations of traditional wireless networks. Leveraging the advancements in OFDMA and mmWave frequencies, further enhances the capabilities of UAV-based communication systems [4], [5].

Recently, cooperative communication between UAVs has been recognized as an effective means of enhancing the performance and coverage of UAV-based networks. By leveraging the spatial diversity and mobility of multiple UAVs, cooperative communication can mitigate the effects of fading channels, extend coverage area, and improve overall system capacity. Furthermore, cooperation among UAVs can enable advanced applications, such as joint beamforming and interference management, leading to improved quality-of-service (QoS) provisions for heterogeneous user requirements [6].

To cooperate effectively, coordination among UAVs must be considered. However, jointly optimizing the operations of multiple UAVs in a centralized manner often result in inherent challenges and limitations. One significant drawback is the high cost associated with backhaul communications and the substantial control overhead required [7], [8]. As the number of UAVs in the network increases, the amount of information exchanged between the UAVs and the central controller escalates rapidly, resulting in excessive communication delays and network congestion. This increased control overhead not only consumes valuable bandwidth resources but also introduces additional latency, which can severely degrade the real-time performance of the system. In scenarios where strict latency requirements exist, such as in mission-critical applications or time-sensitive communications, the centralized approach may not be viable.

In contrast, distributed optimization approaches offer a promising alternative for mitigating the limitations of centralized control architectures [9]. In a distributed optimization framework, each UAV operates autonomously and makes local decisions based on its own information and the information received from neighboring UAVs. This approach eliminates the need for a central controller and the associated backhaul communications, thereby reducing the cost and control overhead significantly [10], [11].

By distributing the optimization process among UAVs, the overall system becomes more scalable and adaptable. Each UAV can independently optimize its resource allocation based on local observations and consider its own objectives and constraints. The distributed nature of the optimization process also enhances the robustness of the system against failures or disruptions in individual UAVs, because the decision-making process is not dependent on a single central entity [12].

However, the distributed nature of this optimization also presents challenges, primarily due to the lack of global information visibility. This is where game theory comes into play. Game theory, especially in the context of communication networks, offers a mathematical tool to model and analyze interactions among rational entities or players. In our work, game theory provides the analytical framework to model, analyze, and solve the distributed subcarrier assignment and discrete power allocation problem. It allows us to capture the independent and often conflicting objectives of each UAV, while also accounting for the inherent network dynamics and heterogeneous QoS requirements.

Recently, game theory has gained substantial attention as a powerful tool to address these challenges [13], [36], [37]. Game theory provides a framework to model the strategic interactions among self-interested UAVs, facilitating the design of distributed algorithms that can achieve optimal resource allocation solutions. By incorporating game-theoretic concepts into the design process, we can harness the self-organizing and adaptive nature of UAV networks while considering the heterogeneity of the QoS requirements.

A well-known game theory-related resource allocation scheme called iterative water-filling (IWF) was first proposed in [14], where a non-cooperative game was used to model the spectrum management problem with each user iteratively maximizing its own rate. This per-user optimization problem is convex and leads to a water-filling solution. For the two-user cases, it was proven that the Nash Equilibrium (NE) exists and the IWF algorithm converges to the NE under certain conditions [15], [16]. Although game theory has already been used in some related works, we emphasize that there may be no equilibrium exist in traditional non-cooperative game [17]. Therefore the use of IWF is limited under such situations. However, one specific game, called potential game, has gained attention owing to its mathematic properties related to NE existence [18].

Although the existing literature has paid much attention to the power allocation to the OFDMA systems, they are all concerned with the continuous power control problem [19], [20]. However, the discrete power control problem has seldom been investigated. We believe that discrete power control is preferred because it offers two main benefits over continuous power control: simplicity and efficiency, and reduced signaling overhead [7]. By adjusting the transmission power at predefined discrete levels, discrete power control reduces the computational complexity, making it more efficient and resource-friendly. Additionally, limited and known power levels lead to reduced signaling overhead, enabling more efficient communication between devices and base stations, making it an attractive choice in various communication scenarios, particularly in cellular networks [7].

Moreover, existing solutions have the disadvantage of causing unfairness to edge users. This inequity stems from

the fact that edge users generally experience higher path loss compared to others, and in the resource allocation process, the network manager tends to favor users in closer proximity to the base station (BS) who have better channel conditions. While some current approaches attempt to address this fairness concern by using network-level criteria such as max-min, they often neglect to consider the specific and distinct needs of individual users [21], [22].

In addition to the drawbacks of the previous literature mentioned above, ensuring the existence of a NE is the most important aspect of all game theory-related research. Traditional potential game theory can be applie to a problem in which one play's strategy does not affect the others' feasibility strategies. As in [18], a potential game is formed called an interference coordination game, and there are no coupled constraints between players so a traditional potential game can be applied. The same situation also holds in [9] and [23], to name a few. Contrary to all these works, our game has coupled constraints among players which makes the problem harder, and the direct application of the traditional potential game is prohibited because other players can change their strategies to trap the current player in the unfeasible region which can not escape whatever strategy it chooses.

A. CONTRIBUTIONS

Different to most existing optimization approaches for multi-UAV, such as [20], [24], and [25], in this paper, we propose a distributed algorithm based on constrained potential game theory principles to address the aforementioned challenges in multi-UAV millimeter-wave cooperative OFDMA networks with heterogeneous QoS consideration. Our algorithm aims to achieve efficient subcarrier assignment and discrete power allocation, ensuring optimal system performance and satisfying the diverse QoS requirements of users. The contributions of this paper are as follows:

1) We proposed a joint optimization problem named Discrete Power and Subcarrier Allocation (DPSA) which jointly optimizes the discrete power and subcarrier allocation. The fairness and QoS are considered. Note that the heterogeneous QoS we considered is similar but harder than [26], which is a convex constraint and easy to handle. In addition, the formulated problem is nonconvex and mixed-integer nonlinear programming (MINP), and thus is NP-hard in general, which is very challenging to solve.
2) Owing to the existence of heterogeneous QoS constraints in DPSA, the ordinary potential game formulation in most literature, which definitely exists at least one NE [27], does not applicable here. Hence, we propose a novel constrained potential game to tackle this problem, named the Subcarrier and Power Resource Efficient Cooperative Potential Game (SRECPG). We analyze the conditions under which a NE exists in our proposed SRECPG game and provide a proof of its existence under these conditions.
3) In contrast to the current research, which uses best response dynamics to deal with one iteration update with each UAV, we proposed the BR-SSO algorithm and the corresponding sequential play algorithm to dramatically decrease the computation burden caused by the exhaustive search. Furthermore, we demonstrate the convergence of the BR-SSO algorithm to a NE is ensured.
4) Extensive simulations are conducted. The results obtained from the simulations validate the effectiveness of the proposed SRECPG and demonstrate its ability to achieve desirable system performance. We analyzed various performance metrics of BR-SSO, including throughput, fairness, and QoS guarantees, and compared them with the exhaustive search and best-play baseline schemes. The simulation results provide insights into the benefits and advantages of our proposed approach for multi-UAV millimeter-wave cooperative OFDMA networks.

Overall, our contributions include the formulation of a non-convex and NP-hard joint optimization problem, introduction of the SRECPG framework tailored for millimeter-wave characteristics, the analysis of NE existence conditions, proof of convergence for the proposed distributed algorithm, and extensive simulations to validate the effectiveness of our approach. Our work provides valuable insights into the design of efficient resource allocation schemes for multi-UAV millimeter-wave networks, considering the heterogeneous QoS requirements.

B. POTENTIAL APPLICATIONS AND OUTLINE

The development and optimization of multi-UAV millimeter-wave cooperative OFDMA networks, especially with a nuanced consideration of heterogeneous QoS, find relevance in a wide array of real-world applications. As technology continues to permeate every facet of modern life, the need for advanced communication infrastructures to support diverse data traffic requirements becomes paramount. Herein, we outline some salient applications for our proposed network model:

- Emergency Response and Disaster Recovery: Catastrophic events, such as earthquakes, hurricanes, or floods, often result in significant infrastructural damage, disrupting traditional communication networks. In such scenarios, multi-UAV networks can swiftly establish a temporary communication bridge. Given the diversity of data, ranging from voice communications among first responders to high-definition video feeds from search and rescue drones, heterogeneous QoS becomes essential to ensure that each data type receives the requisite bandwidth and priority.
- Large-scale Events Broadcasting: Modern events, be they concerts, sports fixtures, or large-scale public gatherings, increasingly rely on technology for enhanced experiences. With augmented reality applications, live streaming, and real-time social media

engagements becoming the norm, there's a burgeoning demand for high-bandwidth, low-latency communication. UAV-assisted networks can supplement existing infrastructures, providing the necessary bandwidth. The heterogeneous QoS consideration ensures smooth streaming for live broadcasts while simultaneously supporting other types of data traffic.

- Precision Agriculture: The agriculture sector is experiencing a technological renaissance, with innovations aiming to optimize yields and resource utilization. UAVs play a pivotal role, offering real-time monitoring of crops, soil health, and environmental conditions. Some data, like high-resolution imagery, demand high bandwidth, while others, like soil moisture readings, have lesser requirements but might need more frequent transmissions. The heterogeneous QoS in our proposed network ensures each data type's optimal transmission, promoting efficient and informed decision-making for farmers.
- Surveillance and Security: For applications like border patrol, crowd monitoring during public events, or even wildlife tracking, UAVs equipped with cameras and sensors can provide real-time feedback to central monitoring stations. The need for high-resolution video feeds, often in real-time, necessitates networks with high data rates and low latencies. Our proposed network model, with its QoS considerations, ensures that video feeds are seamlessly transmitted while concurrently supporting other data types like telemetry or sensor readings.

In summation, the proposed multi-UAV millimeter-wave cooperative OFDMA network, with its nuanced understanding of QoS considerations, finds applications in diverse domains. Its ability to dynamically allocate resources based on data type and requirement ensures optimal utilization, making it a suitable choice for future communication needs.

The remainder of this paper is organized as follows. Section II presents the proposed system model. Section III presents the formulation of the original joint optimization problem. In Section IV, we describe our proposed constrained potential game formulation for the original problem. We introduce some basic assumptions, based on which, we proceed to theoretically prove the existence of NE and the convergence of a sequential play algorithm to a Nash equilibrium. Section V presents simulation results and performance evaluations, and related discussions. Finally, Section VI concludes the paper and discusses future research directions.

II. SYSTEM MODEL

A. NETWORK MODEL

In our study, we consider a downlink scenario of a UAV-based multi-cell Orthogonal Frequency Division Multiple Access (OFDMA) network as shown in Fig. 1. The

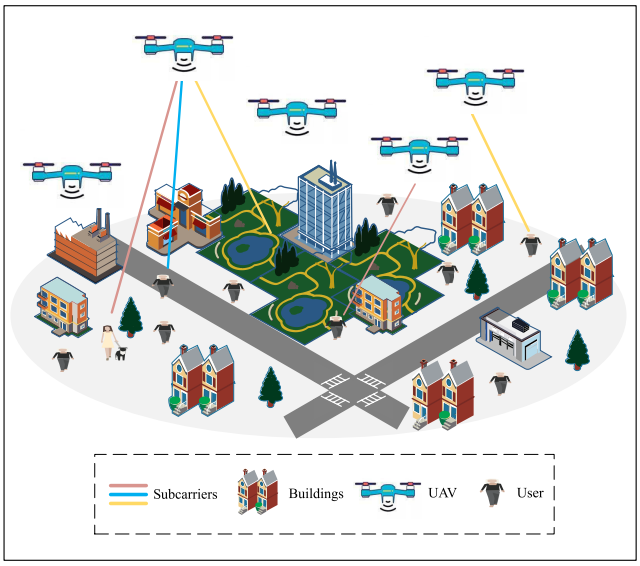

FIGURE 1. System model.

network comprises a set of M coordinated UAVs denoted by $\mathcal{U} = \{1, 2, \ldots, m, \ldots, M\}$ and a set of C Mobile User Equipments (MUEs) denoted by $\mathcal{C} = \{1, 2, \ldots, C\}$. Each MUE is associated with a UAV, and the communication between UAVs and MUEs occurs in a single-hop fashion.

We assume that each UAV cell has a specific set of MUEs, denoted as Ω_i, where i represents the cell index. The total number C of MUEs in the entire system is equal to the sum of the number of MUEs in each UAV cell, given by $|\Omega_i|$, etc, $\mathcal{C} = \cup_{i=1}^{M} \Omega_i$. For simplicity, we assume that each MUE is served by one UAV, and the association is determined based on predefined rules such as received Signal-to-Interference-plus-Noise Ratio (SINR), distance, or manual designation. Hence, there is no overlap between the user sets Ω_i and Ω_j for $i \neq j$. Additionally, we assume $|\Omega_i| = K$ for convenience of the mathematical processing.

The universal frequency reuse deployment is assumed, where the entire spectrum is shared among all the cells. The available spectrum is divided into N orthogonal subchannels, denoted as $\mathcal{N} = \{1, 2, \ldots, n, \ldots N\}$. Each subcarrier has the same bandwidth, which is assumed to be smaller than the coherent bandwidth so that the links are subject to only flat fading and are assigned exclusively to at most one user in each cell, and interferences from adjacent subcarriers or adjacent symbols are assumed to be negligible. The channel conditions and locations of the MUEs and UAVs are further assumed to be static throughout the duration of a gameplay [9].

In the considered system, we define a wireless link from transmitter i to receiver j as (i, j), where i and j belong to the set $\mathcal{U}$ and $\mathcal{C}$, respectively. To represent the subcarrier assignment, we introduce the subcarrier assignment indicator $q_{(i,j)}^{n,\tau}(t)$, which indicates whether subcarrier n is assigned to the wireless link (i, j) at the τth phase in a given time slot t.

It can be defined as follows:

$$q_{i,j}^{n}(t) = \begin{cases} 1, & \text{if subcarrier } n \text{ is assigned to wireless link} \\ & (i,j) \text{ in a time slot t} \\ 0, & \text{otherwise.} \end{cases} \tag{1}$$

Moreover, the channel gains between UAV i and MUE j are represented by the matrix $\mathbf{H}^n$, where $H_{i,j}^n$ represents the channel gain between UAV i and MUE j on subcarrier n.

$$\mathbf{H}^n = \begin{bmatrix} H_{1,1} & H_{1,2} & \dots & H_{1,C} \\ H_{1,1} & \dots & \dots & H_{2,C} \\ \vdots & \vdots & \vdots & \vdots \\ \dots & \dots & \ddots & \dots \\ H_{M,1} & H_{M,2} & \dots & H_{M,C} \end{bmatrix} \tag{2}$$

B. BLOCKAGE MODEL

In the considered network model, we consider the impact of blockages on the UAV-to-user links. The presence of obstacles between the UAVs and ground users can significantly affect the received signal power and hence the overall network performance. We modeled the effect of blockages using a decay factor that modifies the channel gains between UAVs and users in other cells. Although there exist more realistic channel models [38], we use a simplified channel model in this paper because of its mathematical simplicity. We believe that this simplification does not significantly affect the reasonableness of our results, given the focus of our paper.

Let $H_{i,k}^n(t)$ represent the channel gain between UAV i and ground user k at time slot t for the n-th subcarrier. The blockage factor, denoted as $\mathcal{D}_{i,k}$, characterizes the effect of UAV i on the signal received by user k from other cells. We assume that the decay factor $\mathcal{D}_{i,k}$ is a function of the blockage density between the UAV and user, with higher density resulting in more significant blockage effects.

The modified channel gain $\tilde{H}_{i,k}^n(t)$ between UAV i and user k considering the blockage effect is given by:

$$\tilde{H}_{i,k}^n(t) = \frac{1}{\mathcal{D}_{i,k}} \cdot H_{i,k}^n(t) \tag{3}$$

$$\mathcal{D}_{i,k} = \begin{cases} 1, & \text{if } k \in \Omega_i \quad \text{(UAV to its MUE)} \\ \beta_{\text{block}}, & \text{if } k \notin \Omega_i \quad \text{(UAV to other MUEs)} \end{cases} \tag{4}$$

where $\beta_{\text{block}} \in (1, +\infty)$ is a predefined constant reflecting the decay rate, with $\beta_{\text{block}} = 1$ represent the non-blockeage situation and $\beta_{\text{block}} \to +\infty$ refere to the inpenetratable blockages situation, respectively. The blockage factor $\mathcal{D}_{i,k}$ can be determined based on real-world measurements, simulations, or empirical models. It depends on the specific environment, the presence of obstacles, and height and position of the UAV. Furthermore, $\mathcal{D}_{i,k}$ should be updated dynamically to capture the changes in the network environment over time.

It is essential to continuously update $\mathcal{D}_{i,k}$ to capture changes in the network environment, such as UAV mobility and variations in obstacle density. Incorporating the blockage model allows us to more accurately evaluate the performance of the UAV network, considering the potential impact of blockages on the UAV-to-user links and overall system performance. In our study, we used a predefined blockage factor to make sure that our framework was flexible enough to accommodate a variety of different blockage scenarios. The details of blockage factor measurement are out of scope of this paper and can be a topic for future research.

C. SIGNAL MODEL

In our study, we incorporate both line-of-sight (LOS) and nonline-of-sight (NLOS) channel components, consistent with prevailing literature [39], [40], [41]. Our model assumes that the channel gain remains consistent throughout a given time slot. Let's define $H_{i,j}^n(t)$ the channel gain from i to j in time slot t on subcarrier n. It's essential to note that the channels are not necessarily reciprocal, i.e., $H_{i,j}^n(t) \neq H_{j,i}^n(t)$. Then the channel power gain over subcarrier n can be expressed as:

$$H_{i,j}^n(t) = \Phi_{i,j}^n(t) \left| g^n(t) \right|^2 \tag{5}$$

where $\Phi_{i,j}^n(t) = PL_{freespace}$ denote the large-scale fading from i to j during time slot t, $PL_{freespace} = D_t D_r \left(\frac{\lambda}{4\pi d_{i,j}(t)}\right)^{\alpha}$ denotes the free space pathloss and $\alpha \geq 2$ being the pathloss coefficient which ranges from 2 to 6. $D_t = 0\,\text{dBi}$ and $D_r = 0\,\text{dBi}$ is the directivity of the transmitting antenna and the directivity of the receiving antenna, respectively. λ is the signal wavelength. $g^n(t)$ represents the independent and identically distributed Rayleigh freqency-selected small scale fading due to multipath propagation and satisfies $g^n(t) \sim \mathcal{CN}(0, 1)$.

While our current system focuses on frequency-selective Rayleigh fading, each subcarrier in OFDMA is narrow enough to be considered as undergoing flat fading [26]. For future research endeavors, exploring other fading models like Rician [40] or Nakagami [39] might offer additional insights into the channel characteristics.

For the sake of tractability, we follow existing works which broadly assume perfect channel-state information (CSI). To evaluate the performance of the system, we consider the achievable sum rate for each MUE k in cell i. The sum rate is calculated as the logarithm of the signal-to-interference-plus-noise ratio (SINR) and is given by:

$$R_{i,k} = B \sum_{n \in \mathcal{N}} \log \left(1 + \frac{q_{i,k}^n p_i^n(t) \left| H_{i,k}^n(t) \right|^2}{\sum_{\forall j \in \mathcal{U}, j \neq i} \sum_{\forall m \in \Omega_j} q_{j,m}^n p_j^n(t) \left| H_{j,k}^n(t) \right|^2 + \sigma^2} \right) \tag{6}$$

where $p_i^n(t)$ represents the power allocated by UAV i on subcarrier n in time slot t, σ^2 and B are the noise power and subcarrier bandwidth, respectively.

The sum-rate of cell i, denoted as R_i, is the sum of the achievable sum-rates of all the MUEs in that cell and is given by:

$$R_i = \sum_{k \in \Omega_i} R_{i,k} \tag{7}$$

III. JOINT OPTIMIZATION PROBLEM FORMULATION

We formulate the optimization problem for resource allocation in a multi-UAV network with coordinated mobile user equipments (MUEs). The objective is to maximize the sum rate of all MUEs in the network while considering various constraints.

$$\text{DPSA:} \max_{\mathbb{P},\mathbb{Q}} \quad \sum_{i \in \mathcal{U}} R_i \tag{8}$$

$$s.t. \quad R_{i,k} \geq \mathcal{R}_k \quad \forall i \in \mathcal{U}, k \in \Omega_i \tag{9}$$

$$\sum_{j=1}^{C} q_{i,j}^n(t) \leq 1 \quad j \in \Omega_i, \forall i \in \mathcal{U}, \tag{10}$$

$$q_{i,j}^n(t) = \{0, 1\} \quad \forall n \in \mathcal{N}, \forall i \in \mathcal{U}, \forall j \in \Omega_i \tag{11}$$

$$\sum_{n=1}^{N} P_i^n(t) \leq P_{UAV}^{max} \quad \forall i \in \mathcal{U} \tag{12}$$

$$P_i^n(t) \in \Xi, \quad \forall i \in \mathcal{U}$$

$$\Xi \triangleq \{0, \rho P^{max}, 2\rho P^{max} \cdots, P^{max}\} \tag{13}$$

The optimization problem involves maximizing the overall network throughput, defined as the sum rate of all MUEs, while considering the following constraints:

QoS Constraint (9): For each UAV i and its associated MUEs in Ω_i, the achieved data rate should satisfy a minimum rate requirement $\mathcal{R}_k$. This constraint ensures that each MUE experiences a satisfactory service level.

Subcarrier Allocation Constraint (10): The total number of subcarriers allocated to a UAV i for communication with its associated MUEs in Ω_i should not exceed 1. This constraint ensures that only one MUE exists on a specific subcarrier at time t.

Binary Variable Constraint (11): The subcarrier allocation variables $q_{i,j}^n(t)$ are binary and can only take values of 0 or 1. This constraint enforces the discrete nature of subcarrier allocation.

Maximum UAV Power Constraint (12): The total power used by each UAV i for communication with its associated MUEs should not exceed a predefined maximum power P_{UAV}^{max}. This constraint ensures that UAVs operate within their power limits.

Discrete Power Allocation Constraint(13): The transmit power $P_i^n(t)$ used by each UAV i on subcarrier n at time slot t should be selected from a predefined set $\Xi = \{0, \rho P^{max}, 2\rho P^{max}, \ldots, P^{max}\}$, where ρ is a power level factor, and P^{max} is the maximum transmit power. This constraint enforces discrete power allocation to enhance power efficiency. We consider two types of discrete power level sets: exponential power level set and uniform power level set as in [28].

In summary, this joint optimization problem aims to maximize the sum rate of the network while satisfying the minimum rate requirements for MUEs, subcarrier assignment constraints, and power allocation limitations. The solution to this problem will provide efficient resource allocation strategies for the multi-cell OFDMA network, optimizing the performance in terms of achievable rates and overall network capacity.

The joint optimization problem (8) is mixed-integer nonlinear programming (MINP) and is known to be NP-hard in general [29] which is very challenging to solve as the complexity increases at least exponentially with the problem size.

IV. DISTRIBUTED TRANSFORMATION

A. CONSTRAINED POTENTIAL GAME MODEL

We formulated the problem (8) within the framework of game theory. Specifically, we consider a strategic non-cooperative game, in which each player is a UAV, competes against the others and selfishness maximizes its own cell sum rate by choosing the power allocation and subcarrier assignment (i.e., its strategy), while satisfying the QoS constraints of its own cell. However, as the feasibility of QoS constraints of a particular UAV-cell also depends on the strategies selected by the other UAVs, the *traditional potential game approach* such as [9] and [23] does not apply here, because the strategies chosen by the other UAVs can affect the feasibility of its QoS constraints and make them unfeasible, thus equilibrium can not be achieved thereafter. Here we provide some new definitions and solve this problem by using a *constrained potential game approach*.

We denote the set of players $\mathcal{U} = \{1, 2, \ldots, M\}$, which represents the M UAVs. For each UAV i, its available strategy $Q_i = \{P_i, S_i\}$ is a feasible assignment of power and subcarriers to its MUEs. Then, an eligible sub-strategy P_i and S_i of UAV i may be represented by $N \times |\Omega_i|$ matrix as follows:

$$S_i = \begin{bmatrix} s_{1,1} & s_{1,2} & \cdots & s_{1,|\Omega_i|} \\ s_{1,1} & \cdots & \cdots & s_{2,|\Omega_i|} \\ \vdots & \vdots & \vdots & \vdots \\ \cdots & \cdots & \ddots & \cdots \\ s_{n,1} & s_{n,2} & \cdots & s_{n,|\Omega_i|} \end{bmatrix} \tag{14}$$

where $s_{i,j} \in \{0, 1\}, i \in \mathcal{N}, j \in \Omega_i$ indicates the subcarrier i is assigned to j-th MUE of cell i (not the j-th MUE of the system). Similarly, the P_i can be defined as follows:

$$P_i = \begin{bmatrix} p_{1,1} & p_{1,2} & \cdots & p_{1,|\Omega_i|} \\ p_{1,1} & \cdots & \cdots & p_{2,|\Omega_i|} \\ \vdots & \vdots & \vdots & \vdots \\ \cdots & \cdots & \ddots & \cdots \\ p_{n,1} & p_{n,2} & \cdots & p_{n,|\Omega_i|} \end{bmatrix} \tag{15}$$

where $p_{i,j} \in \Xi, i \in \mathcal{N}, j \in \Omega_i$ indicates the subcarrier i is assigned to j-th MUE of cell i (not the j-th MUE of the system). Let the strategy set $\mathbb{Q}_i$ denote the set of all possible combinations that Q_i can take, that is $Q_i \subseteq \mathbb{Q}_i$. Moreover, a strategy profile $\mathbf{Q}$ can be understood as the joint strategy of all players, that is, $\mathbf{Q} = (Q_i, \mathbf{Q}_{-i})$, where $Q_{-i} \subseteq \mathbb{Q}_{-i}$. The domain of $\mathbb{Q}$ is called the strategy space and is defined by $\mathbb{Q} = \mathbb{Q}_1 \times \ldots \times \mathbb{Q}_M$.

There are multiple definitions of NE exist according to [30], such as Satisfaction Equilibrium, social equilibrium, and generalized Nash equilibrium, in order to make our manuscript more strict, we give a rigorous definition of NE and GNE as follows:

Definition 1: A strategy profile $\mathbf{Q}^* = \left(\mathbf{Q}_1^*, \mathbf{Q}_2^*, \ldots, \mathbf{Q}_M^*\right)$ is a NE if and only if

$$U_m\left(Q_m^*, \mathbf{Q}_{-m}^*\right) \geq U_m\left(Q_m, \mathbf{Q}_{-m}^*\right), \forall m \in \mathcal{U},$$

where $M = |\mathcal{U}|$ denotes the cardinality of $\mathcal{U}$, $\mathbf{Q}_{-m}^* = \left(\mathbf{Q}_1^*, \mathbf{Q}_2^*, \ldots, \mathbf{Q}_{m-1}^*, \mathbf{Q}_{m+1}^*, \ldots, \mathbf{Q}_M^*\right)$ are the strategies selected by all the other players except m. NE indicates no one has the intention to change its strategy since it cannot increase its utility unilaterally [23].

A NE of the game is reached when each UAV, given the strategy profile of the others, does not get any sum rate increase by unilaterally changing its own strategy, still keeping the QoS constraints satisfied. Stated in mathematical terms, the game has the following structure:

$\mathbf{P}_i$ and $\mathbf{S}_i$ are the power and subcarrier strategy sets of user i, and $U_i(\cdot)$ is the i th user utility function. Each user selects a power level P_i such that $P_i \in \mathbf{P}_i$ and a subcarrier assignment S_i such that $S_i \in \mathbf{S}_i$. Let the power vector $\mathbf{P} = (P_1, \ldots, P_N) \in \overrightarrow{\mathbf{P}}$ denote the outcome of the game in terms of the selected power levels for all users, where $\overrightarrow{\mathbf{P}}$ is the set of all feasible power vectors. Furthermore, let the subcarrier vector $\mathbf{S} = (W_1, \ldots, W_N) \in \overrightarrow{\mathbf{S}}$ denote the outcome of the game in terms of the selected subcarrier shares of all users, where $\overrightarrow{\mathbf{S}}$ is the set of all feasible subcarrier vectors. The resulting utility for the i th user is $U_i\left(\mathbf{P}, \mathbf{S}; (\Pi_P, \Pi_W)\right)$. An alternative notation $U_i\left(\mathbf{P}_i, \mathbf{S}_i, \mathbf{P}_{-i}, \mathbf{S}_{-i}; (\Pi_P, \Pi_W)\right)$ can also be used to emphasize that the i th user has control only over its own power and subcarrier strategies $\mathbf{P}_i$ and $\mathbf{S}_i$, respectively. In this sense, $\mathbf{S}_{-i}$ and $\mathbf{P}_{-i}$ denote vectors consisting of elements of the power $\mathbf{P}$ and the subcarrier $\mathbf{S}$ excluding the i th element.

Definition 2: A constrained potential game $\mathcal{G}$ is the N players non-cooperative game with payoff vector

$$\mathcal{G} = \left[\mathcal{U}, \{\mathbf{Q}_k\}_{k\in\mathbb{U}}, \{U_k\}_{k\in\mathcal{U}}, \{f_k\}_{k\in\mathcal{U}}\right] \tag{16}$$

where $\mathcal{U} = \{1, 2, \ldots, m, \ldots, M\}$ is the set of players (i.e., UAVs), $\mathcal{Q}_l = \mathcal{S}_l \otimes \mathcal{P}_l$ is the set of available joint power and subcarrier allocation strategy for player l, and U_l is the utility function of player l. where $\mathcal{S}_k = \{0, 1\}$ is the available subcarrier switching strategy for player k, U_k is the utility function of player k, and f_k represents a correspondence function for satisfaction of the constraint. An strategy profile of all the players is a vector, denoted by $\mathbf{Q} = (Q_1, Q_2, \ldots, Q_K) \in \mathcal{Q}$, where $\mathcal{Q} = \mathcal{Q}_1 \otimes \mathcal{Q}_2 \otimes \cdots \otimes \mathcal{Q}_K$ represents the joint strategy space for all the players. Besides, the strategy profile of all the players excluding k is denoted by $\mathbf{Q}_{-k} = (Q_1, \ldots, Q_{k-1}, Q_{k+1} \ldots, Q_K) \in \mathcal{Q}_{-k}$, where $\mathcal{Q}_{-k} = \mathcal{Q}_1 \otimes \cdots \otimes \mathcal{Q}_{k-1} \otimes \mathcal{Q}_{k+1} \otimes \cdots \otimes \mathcal{Q}_K$.

$$f_i\left(\mathbf{Q}_{-i}\right) \triangleq \{Q_i \subseteq \Psi, \quad R_i(Q_i, \mathbf{Q}_{-i}) \succcurlyeq \mathcal{R}_i\}$$

where Ψ is the feasible space which satisfy the constraints (10)-(13), obviously $\Psi \subseteq \mathbb{R}_+^{2MN}$. $\mathcal{R}_i$ is the QoS minimum rate requirement vector in cell i where $\mathcal{R}_i \subseteq \mathbb{R}_+^{\Omega_i}$.

As in the mmWave network, we can assume the interference from other UAVs is negligible owing to the distance and blockages. So we can assume SINR $\gg 1$ (Specifically when the SNIR is low, the following approximation obtained by Taylor expansion holds [31] : $\log_2(1 + \text{SNIR}) \approx \frac{\text{SNIR}}{\ln 2}$.), then (7) can be transformed to the following:

$$\tilde{R}_i = B \sum_{k\in\Omega_i} \sum_{N\in\mathcal{N}} \log \times \left(\frac{q_{i,k}^n p_i^n(t) \left|H_{i,k}^n(t)\right|^2}{\sum_{\forall j\in\mathcal{U}, j\neq i} \sum_{\forall m\in\Omega_j} q_{j,m}^n p_j^n(t) \left|H_{j,k}^n(t)\right|^2 + \sigma^2} \right) \tag{17}$$

The unity function of cell i is defined as

$$U_i(Q_i, \mathbf{Q}_{-i}) = \tilde{R}_i \tag{18}$$

$$= \varphi_i(Q_i) - \chi_i(\mathbf{Q}_{-i}) \tag{19}$$

where $\varphi_i(Q_i) = B \sum_{k\in\Omega_i} \sum_{N\in\mathcal{N}} \log(q_{i,k}^n p_i^n(t) \left|H_{i,k}^n(t)\right|^2)$, $\chi_i(\mathbf{Q}_{-i}) = B \sum_{k\in\Omega_i} \sum_{N\in\mathcal{N}} \log(\sum_{\forall j\in\mathcal{U}, j\neq i} \sum_{\forall m\in\Omega_j} q_{j,m}^n p_j^n(t) \left|H_{j,k}^n(t)\right|^2 + \sigma^2)$. Q_i is the power and subcarrier allocation strategy of user i, $\mathbf{Q}_{-i}$ contains the strategies of all the other users. Obviously, the game is an identical-interest game.

Then the UAV cooperate sum rate game can be expressed as:

$$\max_{Q_i} U_i(Q_i, \mathbf{Q}_{-i}) \tag{20}$$

$$s.t. Q_i \subseteq f_i\left(\mathbf{Q}_{-i}\right) \tag{21}$$

The GNE under pure strategy in games of normal form with a constrained set of actions can be defined as follows:

Definition 3 (Generalized Nash Equilibrium): A UAV allocation profile $\mathbf{Q}^*$ is a pure strategy GNE of the game if and only if

$$\forall i \in \mathcal{M}, Q_i \subseteq f_i\left(\mathbf{Q}_{-i}\right) \tag{22}$$

$$U_i(Q_i^*, \mathbf{Q}_{-i}) \geq U_i(Q_i, \mathbf{Q}_{-i}) \tag{23}$$

Let us define $\mathcal{F}_k = \{(Q_k, \mathbf{Q}_{-k}) : Q_k \in f_k\left(\mathbf{Q}_{-k}\right)\}$. The set $\mathcal{F}_k$ determines the action profiles which can be observed as outcomes of the game $\mathcal{G}$, when only player k is allowed to play actions belonging to the set $f_k\left(\mathbf{Q}_{-k}\right)$ given any action profile $\mathbf{Q}_{-k}$. Then, $\hat{\mathcal{F}} = \bigcup_{k\in\mathcal{M}} \mathcal{F}_k$ contains all possible unilateral deviations, while $\mathcal{F} = \bigcap_{k\in\mathcal{M}} \mathcal{F}_k$ corresponds to

the set of all possible (feasible) outcomes of the game $\mathcal{G}$. Notably, the definition of $\mathcal{F}$ coincides with the constraint (22) for the GNE.

Definition 4: (Sum Rate Exact Constrained Potential Game (SRECPG)): The sum rate game $\mathcal{G} = \left[\mathcal{U}, \{\mathbf{Q}_k\}_{k\in\mathbb{U}}, \{U_k\}_{k\in\mathcal{U}}, \{f_k\}_{k\in\mathcal{U}}\right]$ is an exact constrained potential game if there exists a function $\Phi : \hat{\mathcal{F}} \to \mathbb{R}$ such that for all $\mathbf{Q} \in \hat{\mathcal{F}}$, it holds that, $\forall k \in \mathcal{M}$, and $Q_k \subseteq f_k(\mathbf{Q}_{-k})$

$$U_k\left(Q_k', \mathbf{Q}_{-k}\right) - U_k\left(Q_k, \mathbf{Q}_{-k}\right) = \Phi\left(Q_k', \mathbf{Q}_{-k}\right) - \Phi\left(Q_k, \mathbf{Q}_{-k}\right)$$

The function Φ is called an exact potential function for the constrained game $\mathcal{G}$.

Theorem 1: The sum rate game $\mathcal{G} = \left[\mathcal{U}, \{\mathbf{Q}_k\}_{k\in\mathbb{U}}, \{U_k\}_{k\in\mathcal{U}}, \{f_k\}_{k\in\mathcal{U}}\right]$ is an exact constrained potential game.

Proof 1: First, we construct a potential function as

$$\Phi\left(Q_k, \mathbf{Q}_{-k}\right) = \sum_{i\in\mathcal{U}} \varphi_i(Q_i) \quad s.t.\ (22) \tag{24}$$

Suppose that an arbitrary player, say k, unilaterally changes its strategy from Q_k to $Q_{k'} \subseteq f_k(\mathbf{Q}_{-k})$, then the change of the potential function caused by this unilateral change is given by

$$\begin{aligned}
&\Phi\left(Q_{k'}, \mathbf{Q}_{-k}\right) - \Phi\left(Q_k, \mathbf{Q}_{-k}\right) \\
&= \varphi_k\left(Q_{k'}\right) + \sum_{j\neq k} \varphi_j\left(Q_j\right) - \varphi_k\left(Q_k\right) - \sum_{j\neq k} \varphi_j\left(Q_j\right) \\
&= \varphi_k\left(Q_{k'}\right) - \varphi_k\left(Q_k\right)
\end{aligned} \tag{25}$$

At the same time,

$$\begin{aligned}
&U_k\left(Q_k', \mathbf{Q}_{-k}\right) - U_k\left(Q_k, \mathbf{Q}_{-k}\right) \\
&= \varphi_k(Q_k') - \chi_k(\mathbf{Q}_{-k}) - \varphi_k(Q_k) + \chi_k(\mathbf{Q}_{-k}) \\
&= \varphi_k\left(Q_{k'}\right) - \varphi_k\left(Q_k\right)
\end{aligned} \tag{26}$$

In other words, the change in individual utility function caused by any player's unilateral deviation is equal to the change in the potential function. Thus, according to the definition, G is an exact constrained potential game. This concludes the proof.

B. NASH EQUILIBRIUM ANALYSIS

Theorem 2 (Existence): The exact constrained potential game $\mathcal{G} = \left[\mathcal{U}, \{\mathbf{Q}_k\}_{k\in\mathcal{U}}, \{U_k\}_{k\in\mathcal{U}}, \{f_k\}_{k\in\mathcal{U}}\right]$ with potential function $\Phi : \hat{\mathcal{F}} \to \mathbb{R}$, has at least one GNE in pure strategy if the following sufficient conditions satisfied:

$$N \geq \max|\Omega_i| \qquad \forall i \in \mathcal{M} \tag{27}$$

$$P_{min}(t) \geq \frac{(MP^{max}\left|H_{max}(t)\right|^2 + \sigma^2)e^{\mathcal{R}_{min}}}{\left|H_{min}(t)\right|^2} \tag{28}$$

where $H_{min}(t) = \min H_{i,k}^n(t), \forall n \in \mathcal{N}, i \in \mathcal{M}, k \in \Phi_i$, $H_{max}(t) = \max H_{i,k}^n(t), \forall n \in \mathcal{N}, i \in \mathcal{M}, k \notin \Phi_i$, $H_{min}(t) \gg H_{max}(t)$ in high SINR regime. $P_{min}(t) \in \Xi\backslash\{0\}$ is the lowest power of the total discrete power set Ξ excluded the zero element and $\mathcal{R}_{min} = \min \mathcal{R}_k, \forall k \in \mathbb{C}$.

Proof 2: First, we prove there exists at least one the feasible outcome for the game As we are in high SINR, we have

$$\begin{aligned}
&\sum_{N\in\mathcal{N}} \log\left(1 + \frac{q_{i,k}^n p_i^n(t)\left|H_{i,k}^n(t)\right|^2}{\sum_{\forall j\in\mathcal{U}, j\neq i}\sum_{\forall m\in\Omega_j} q_{j,m}^n p_j^n(t)\left|H_{j,k}^n(t)\right|^2 + \sigma^2}\right) \\
&\geq \sum_{N\in\mathcal{N}} \log\left(\frac{q_{i,k}^n p_i^n(t)\left|H_{i,k}^n(t)\right|^2}{\sum_{\forall j\in\mathcal{U}, j\neq i}\sum_{\forall m\in\Omega_j} q_{j,m}^n p_j^n(t)\left|H_{j,k}^n(t)\right|^2 + \sigma^2}\right) \\
&\geq \log\left(\frac{q_{i,k}^n p_i^n(t)\left|H_{i,k}^n(t)\right|^2}{\sum_{\forall j\in\mathcal{U}, j\neq i}\sum_{\forall m\in\Omega_j} q_{j,m}^n p_j^n(t)\left|H_{j,k}^n(t)\right|^2 + \sigma^2}\right) \\
&\geq \log\left(\frac{q_{i,k}^n p_i^n(t)\left|H_{i,k}^n(t)\right|^2}{MP^{max}\left|H_{max}(t)\right|^2 + \sigma^2}\right) \\
&\geq \log\left(\frac{P_{min}(t)\left|H_{min}(t)\right|^2}{MP^{max}\left|H_{max}(t)\right|^2 + \sigma^2}\right) \geq \mathcal{R}_{min}
\end{aligned} \tag{29}$$

After some math manipulation, (29) can be transformed as:

$$P_{min}(t)\left|H_{min}(t)\right|^2 \geq (MP^{max}\left|H_{max}(t)\right|^2 + \sigma^2)e^{\mathcal{R}_{min}} \tag{30}$$

Then it is easily seen the following:

$$P_{min}(t) \geq \frac{(MP^{max}\left|H_{max}(t)\right|^2 + \sigma^2)e^{\mathcal{R}_{min}}}{\left|H_{min}(t)\right|^2} \tag{31}$$

We can seen $S_i[j,k] = \begin{cases} 1, & (j=k) \\ 0, & \text{otherwise.} \end{cases}$, $P_i[j,k] = \begin{cases} P_{min}(t), & (j=k) \\ 0, & \text{otherwise.} \end{cases}$ is a feasible solution, i.e., $\{\mathbf{Q}_i\}_{i\in\mathcal{U}} = \{P_i, S_i\} \in \mathcal{F}$. Thus, there exists at least one the feasible outcome for the game.

Then the first part of theorem is proved. Next, we will prove the second part.

Now, $\forall k \in \mathcal{K}$, any unilateral deviation of player k from $\mathbf{Q}^0$ leads to an action profile $\mathbf{Q}' = \left(Q_k', \mathbf{Q}_{-k}\right) \in \mathcal{F}_k$, i.e., $Q_k' \in f_k(\mathbf{Q}_{-k})$. Because the correspondence function f_k is defined to guarantee that the QoS constraints are satisfied in its cell, the unilateral deviation from a feasible action profile $\mathbf{Q}^0$ is also a feasible action profile. Thus, $\mathbf{Q}^1 = \left(Q_k', \mathbf{Q}_{-k}\right) \in \mathcal{F}$. Moreover, since $Q_k' \in f_k(\mathbf{Q}_{-k})$, according to Theorem 1, we have:

$$\begin{aligned}
&U_k\left(Q_k', \mathbf{Q}_{-k}\right) - U_k\left(Q_k, \mathbf{Q}_{-k}\right) \\
&= \Phi\left(Q_k', \mathbf{Q}_{-k}\right) - \Phi\left(Q_k, \mathbf{Q}_{-k}\right)
\end{aligned} \tag{32}$$

Therefore, $U_k\left(s_k', \mathbf{s}_{\mathcal{D}_k}\right) \geq U_k\left(s_k, \mathbf{s}_{\mathcal{D}_k}\right)$ results in $\Phi\left(s_k', \mathbf{s}_{-k}\right) \geq \Phi\left(s_k, \mathbf{s}_{-k}\right)$. Furthermore, owing to the nature of game, player k unilaterally deviates its strategy from the original strategy s_k to s_k' only when $U_k\left(s_k', \mathbf{s}_{\mathcal{D}_k}\right) \geq U_k\left(s_k, \mathbf{s}_{\mathcal{D}_k}\right)$. Hence, we have $\Phi\left(s_k', \mathbf{s}_{-k}\right) \geq \Phi\left(s_k, \mathbf{s}_{-k}\right)$, i.e., $\Phi\left(\mathbf{s}^1\right) \geq \Phi\left(\mathbf{s}^0\right)$. In this way, unilateral deviations of all the players would achieve such a feasible improvement path

$\{\mathbf{s}^0, \mathbf{s}^1, \mathbf{s}^2, \ldots\} \subseteq \mathcal{F}$, which conforms to $\Phi(\mathbf{s}^0) \leq \Phi(\mathbf{s}^1) \leq \Phi(\mathbf{s}^2) \leq \cdots$.

In addition, because the number of feasible strategy profiles is finite $(|\mathcal{F}| \leq 2^{|\mathcal{K}|})$, the above improvement path must be finite and terminate in one pure strategy GNE point $\mathbf{s}^*$, where no player could unilaterally deviate to increase its utility, still keeping all the system QoS constraints satisfied. Moreover, each GNE maximizes the potential function Φ in the feasible region, either locally or globally.

Theorem 3: For the formulated exact constrained potential games G, each GNE locally or globally maximizes the network sum rate under the QoS constraints, and the best GNE is the global optimum for maximizing the network sum rate.

Proof 3: According to the definition of GNE, for an arbitrary GNE $\mathbf{Q}^*$, we have $Q_i{}^* \subseteq f_i(\mathbf{Q}^*_{-i})$. Then, based on the definition of correspondence f_i, we know that all the GNE are in the feasible region. Besides, we have proved in Theorem 2 that all GNE are the maximizers of the potential function Φ in the feasible region, either locally or globally. Furthermore, according to Eq. 17, when GNE is reached, the sum of all the players' utility functions is approximately equal to the sum rate of the network in high SINR regime. In addition, maximizing the potential function Φ is equal to maximizing the sum rate of the network. Therefore, each GNE of the game G locally or globally maximizes the network sum rate under the QoS constraints and the best GNE is the global optimum for maximizing the network sum rate.

C. BETTER RESPONSE DYNAMICS BASED ON BR-SSO

Definition 5: For player k, the best response strategy Q_k is

$$Q_k = \arg\max_{Q \in \mathbb{Q}_\mathbf{i}} \quad U_i(Q_i, \mathbf{Q}_{-i}) \tag{33}$$

For one play k, selecting the best strategy requires enumerating all the states in state space $\mathbb{Q}_k$. This is formidable even when k is not large, in the following, we provide some lemmas and theorems to illustrate the motivation of using BR-SSO better response dynamics to decrease the complexity of best response play.

Definition 6: ($\Im$ matrix) is a $N \times |\Omega_i|$ matrix. For all the MUEs in a UAV cell i, we can compare the elements in the $\Im$ matrix to decide which link is most appropriate to increase the power level among all the other links.

Lemma 1: For player i, give all the other players' strategies, the best response transmit power vector $\mathbf{P}_i^*$ will have at least one component equal to P_{max} if all the other players are not changing their current feasibility status.

Proof 4: First, we define a level-up operator π as $\pi(P_k) = \begin{cases} P_k + \rho P_{max}, & \forall i \in \mathcal{M}, Q_i \subseteq f_i(\mathbf{Q}_{-i}) \\ P_k, & \text{otherwise.} \end{cases}$. From (7) we have that, for $\mathbf{P}_i \in \mathbb{P}$:

$$\begin{aligned} &R_i(\pi(\mathbf{P}_i)) \\ &= \sum_{k \in \Omega_i} \sum_{N \in \mathcal{N}} \\ &\times \log\left(1 + \frac{q^n_{i,k}\pi(p^n_i(t))\left|H^n_{i,k}(t)\right|^2}{\sum_{\forall j \in \mathcal{U}, j \neq i} \sum_{\forall m \in \Omega_j} q^n_{j,m} p^n_j(t)\left|H^n_{j,k}(t)\right|^2 + \sigma^2}\right) \\ &\geq R_i(\mathbf{P}_i) \end{aligned} \tag{34}$$

Thus, we can always increase the sum rate R_i, by increasing all components of $\mathbf{P}_i$ by one level using the level-up operator π, until one component hits the boundary P^{max} or one of the other player's strategy feasibility is violated. Hence, the best response will have at least one component equal to P^{max}, if all the other players are not changing their current feasibility status as the result of the current player's strategy change.

Definition 7: (Subcarrier Switch Operator (SSO)): is a switch operator on the subcarrier assignment vector of a UAV i which satisfy the following equations:

$$SSO(S_i) = swap(S_i[i, k'], S_i[i, k]) \tag{35}$$

$$\begin{aligned} &\frac{\left|H^n_{i,k'}(t)\right|^2}{\sum_{\forall j \in \mathcal{U}, j \neq i} \sum_{\forall m \in \Omega_j} q^n_{j,m} p^n_j(t)\left|H^n_{j,k'}(t)\right|^2 + \sigma^2} \\ &\geq \frac{\left|H^n_{i,k}(t)\right|^2}{\sum_{\forall j \in \mathcal{U}, j \neq i} \sum_{\forall m \in \Omega_j} q^n_{j,m} p^n_j(t)\left|H^n_{j,k}(t)\right|^2 + \sigma^2}, \end{aligned} \tag{36}$$

$$S_i[i, j'] = 0, S_i[i, j] = 1, Q_i \subseteq f_i(\mathbf{Q}_{-i}) \quad \forall i, \forall j, \tag{37}$$

It can be seen the SSO always makes the MUE that has the best subcarrier gain obtain as many subcarriers as possible with the other MUEs satisfying QoS constraints.

Proposition 1: With the strategies of other players' being fixed, that is, $\mathbf{Q}_{-\mathbf{i}}$, the payoff of player i can be improved, that is, $U_i(Q'_i, \mathbf{Q}_{-i'}) \geq U_i(Q_i, \mathbf{Q}_{-i})$, if we use SSO on the subcarrier policy of it, that is, $S'_i = SSO(S_i)$.

Proof 5: Let us assume two subcarriers of MUE j and k is switched after the SSO, from (17) we can easily derive:

$$\tilde{R}_{i,k} \geq \tilde{R}_{i,j} \tag{38}$$

then according to (7), we can concluded that $\tilde{R}_k \geq \tilde{R}_{kj}$, which proved the proposition.

Based on the above analysis, we propose our Better Response algorithm based on SSO(BR-SSO) for player k. First, we update the subcarrier policy in player k through SSO, then the $\Im$ matrix is formed based on the result matrix of SSO. The algorithm is then iterated through the $\Im$ matrix to select the best subcarrier to increase the power level. If the power does not reach the maximum on the currently selected subcarrier, we will keep leveling up until it reaches the maximum or the total power constraint is violated. Finally, the operated link is deleted from $\Im$ matrix and the second best link will be selected to do the same operations, the whole process will end until all the suitable links are operated or the violation of power constraint

D. ITERATIVE ALGORITHM TO FIND NE

We now address the method used to obtain the NE solution. As stated in theorem 2, convergence for SRECPG is ensured and can be obtained through a sequential best-response dynamic among the players. The algorithm 2 summarizes the steps of the algorithm.

Algorithm 1 Better Response Algorithm Based on SSO(BR-SSO) for Player k

Require: initial strategy Q_k^0; MUE index $h = 0$; Subcarrier index $n = 1$; P^{max}, P_{UAV}^{max}
Ensure: feasible $Q_k^f = \{S_k^f, P_k^f\}$
1: update the subcarrier policy in player k through SSO: $S_k^0 = SSO(S_k^0)$
2: obtain the $\Im$ matrix
3: **while** $n! = N$ **do**
4: find the index h of the maximum element in $\Im\{n\}$
5: **if** $P_k[n,h] \leq P^{max}$ **then**
6: **while** $\sum_{n=1}^{N} P_k[n,h] + \rho P^{max} \leq P_{UAV}^{max}$ **do**
7: $P_k[n,h] = \pi(P_k[n,h])$
8: **end while**
9: **end if**
10: **if** $P_k[n,h] > P^{max}$ **then**
11: break
12: **end if**
13: $n = n + 1$
14: Update $\Im$ by removing element $\{n,h\}$
15: **end while**

We initialize the game with a random subcarrier assignment and power allocation for each player. This is likely to be a non-equilibrium state, and the first player will take action to search for improvement in utility value by looking for a better response strategy based on SSO after observing the opponent's response.

Theorem 4: The iterative process of Algorithm 2 converges to a GNE of the game, namely, a stationary point of the sum rate maximization problem (8).

Proof 6: The proof is similar to the proof in [32], so is omitted here.

V. COMPUTATIONAL COMPLEXITY ANALYSIS

In this section, we introduce the computational complexities of both the best response dynamics based on local exhaustive search (BRLES) and BR-SSO dynamics, followed by a comparative overview. Subsequently, we delve into an in-depth analysis of the sequential play algorithm 2 in the context of these dynamics. To conclude, we provide a summary and highlight key observations drawn from our study.

First, we have the following assumption:

- There are N subcarriers.
- $|\Omega_i|$ is the number of users in UAV cell i.

Algorithm 2 Sequential Play Algorithm

Require: maximum number of iterations $Iter_{max}$; iteration index $i = 0$; player index $k = 1$; P_{MAX},P_{uav}^{Max}, P_{BS}^{Max}
Ensure: feasible $Q^f = \{S^f, P^f\}$
1: select the update order monotonic increasing with player index k
2: set the initial strategy $\mathbf{Q^0}$ according to theorem 2
3: **repeat**
4: **while** $k! = M$ **do**
5: update Q_k^i according to algorithm 1
6: $\mathbf{Q}_k^{i+1} = Q_k^i$
7: $k = k + 1$
8: **end while**
9: **if** $\mathbf{Q^{i+1}} == \mathbf{Q^i}$ **then**
10: Convergence=True
11: **else**
12: Convergence=False
13: $i = i + 1$
14: $k = 1$
15: **end if**
16: **until** Convergence=True OR $Iter_{max}$ is reached

- Each subcarrier has discrete power levels taken from the set Ξ, and the size of this set is $|\Xi| = \frac{P^{\max}}{\rho P^{\max}} + 1$, due to the increments of $\rho P^{\max}$ up to $P^{\max}$.

A. COMPLEXITY OF BR-SSO DYNAMICS

First, we analyze the complexity of BR-SSO dynamics algorithm 1 in detail as follows:

1) **Initialization:** The initial strategy can be set according to theorem 2 which has the complexity of $O(1)$.
2) **Step 1 (SSO):** The complexity of the SSO involves checking conditions for each potential switch. Each subcarrier is compared with every other, then the complexity is $O(N^2)$. Furthermore, SSO should consider the different power levels in Ξ. In a worst-case scenario, where each potential switch checks each power level, the complexity could rise to $O\left(N^2 \times |\Xi|\right)$.
3) **Step 2 (Obtaining the $\Im$ matrix):** Based on the SSO result, we can formulate $\Im$ matrix with the complexity of $O\left(N \times |\Omega_i|\right)$.
4) **Steps 3-15 (Main Loop):**
   - The 'While' loop's iterations are determined by the subcarrier index n. Assuming it iterates N times in the worst case, its complexity is $O\left(N\right)$.
   - Step 4: Finding the index h of the maximum element can be done in $O(N \times |\Omega_i|)$.
   - Steps 6-8: Given the power levels, the inner while loop for updating the power might run up to $|\Xi|$ times in the worst case, making its complexity $O\left(|\Xi|\right)$.
   - Steps 10-14: The complexity is $O(1)$.

   Combining the loop structures we can compute the complexity of the main loop as: $O\left(N \times (|\Omega_i| \times N + |\Xi|\right)$.

Based on the above analysis, we can deduce the total complexity of BR-SSO dynamics as follows:

$$\begin{aligned} O_{\text{BR-SSO}} = & O\left(N^2 \times |\Xi|\right) \\ & + O\left(N \times |\Omega_i|\right) \\ & + O\left(N \times (|\Omega_i| \times N + |\Xi|\right) \end{aligned}$$

This is an upper-bound estimate for the worst-case scenario. Actual run-times might be lesser depending on specific conditions and optimization measures applied to the implementation of the algorithm.

B. COMPLEXITY OF BRLES DYNAMICS

Next, we analylize the complexity of BRLES dynamcis. The BRLES is a local exhausted search method which will enumerate all local states of current UAV player's strategy space. So we can come up with the following two aspects:

- **Subcarrier Assignments:** Each of the N subcarriers can be assigned to any of the $|\Omega_i|$ users or remain unassigned. This leads to $(|\Omega_i| + 1)$ possibilities for each subcarrier. So, for all subcarriers, the possibilities become $(|\Omega_i| + 1)^N$.
- **Power Assignments:** For each subcarrier-user assignment, the power level on that subcarrier can take any value from the set Ξ. Given the power level set, there are $|\Xi|$ possible power levels, so the possibilities for all subcarriers are $|\Xi|^N$.

Combining subcarrier and power assignments for each UAV, the total possibilities are: $(|\Omega_i| + 1)^N \times |\Xi|^N$.

For exhaustive search, each possibility must be evaluated, so the complexity for a single UAV is $O\left((|\Omega_i| + 1)^N \times |\Xi|^N\right)$.

However, if there are multiple UAVs, the total complexity remains the same since each UAV explores its own local search space exhaustively.

In summary, the BRLES complexity for a single UAV i is: $O_{\text{BRLES}} = O\left((|\Omega_i| + 1)^N \times |\Xi|^N\right)$. It's worth noting that this complexity can grow very quickly as N or $|\Omega_i|$ increases, making the algorithm computationally demanding.

C. COMPLEXITY COMPARISON

Now we give the detailed comparison of BRLES and BR-SSO complexities from different aspects.

1) **Growth with Respect to N (Subcarriers):**
   - In BR-SSO, the complexity grows polynomial with the number of subcarriers N. As the number of subcarriers increases, the time taken by BR-SSO would increase in a polynomial fashion.
   - In BRLES, the growth is exponential with respect to N. Even a small increase in N can cause a significant increase in complexity, making the algorithm computationally very expensive.
2) **Growth with Respect to $|\Omega_i|$ (Users in UAV cell i):**
   - In BR-SSO, the complexity grows linearly with the number of users in the UAV cell. So, the more users you have in a given cell, the longer it will take to compute, but the growth is predictable and manageable.
   - In BRLES, the complexity grows exponentially with the number of users. This means that adding even a few users can drastically increase the time taken by the algorithm. If the number of users is large, this method might not be practical.
3) **Growth with Respect to $|\Xi|$ (Power Levels):**
   - Both algorithms have a similar growth pattern with respect to $|\Xi|$. In BR-SSO, it grows linearly, and in BRLES, it grows exponentially with N, but the base of the exponential growth is determined by $|\Xi|$.
4) **Practical Implications:**
   - *Scalability:* BR-SSO is much more scalable than BRLES. As the system parameters like the number of subcarriers or users increase, BR-SSO remains computationally feasible, while BRLES quickly becomes impractical.
   - *Solution Quality:* While BR-SSO is computationally more efficient, it may not always find the global optimal solution since it uses a heuristic search. On the other hand, BRLES, being an exhaustive search, will always find the global optimal solution if given enough time. This implies a trade-off between solution quality and computational efficiency.
   - *Real-time Applications:* For real-time applications where computational efficiency is crucial, BR-SSO would be more suitable. BRLES might be more appropriate for scenarios where obtaining the global optimum is critical, and computational resources/time are abundant.

D. COMPLEXITY OF SEQUENTIAL PLAY ALGORITHM

We then analyze the complexity of our sequential play algorithm 2 when choosing the BR-SSO and BRLES dynamics, respectively, as follows:

1) **Initialization:**
   - The initialization steps, including setting the iteration index, player index, and other parameters, have constant time complexities, represented as $O(1)$ operations.
   - Setting the initial strategy according to theorem 2 has a complexity denoted as $O(1)$.
2) **Main Iterative Process:**
   - The algorithm comprises nested loops: an outer 'repeat-until' loop and an inner 'while' loop.
3) **Inner While Loop:**
   - This loop iterates over all players (UAVs), totaling M. Thus, this loop runs M times.
   - Inside this loop, the most intensive computational step is the strategy update using either the BR-SSO algorithm or BRLES. Depending on which algorithm is applied, the complexity varies.

4) **Outer Repeat-Until Loop:**
   - This loop's iteration count isn't explicitly detailed, but it continues until convergence. In a worst-case scenario, it runs for the maximum iteration count, represented as $\text{Iter}_{\max}$.
5) **Aggregated Complexity:**
   - With the BR-SSO strategy update, the overall complexity is $O(\text{Iter}_{\max} \times M \times O_{\text{BR-SSO}})$, where $O_{\text{BR-SSO}} = O\left(N^2 \times |\Xi|\right) + O\left(N \times |\Omega_i|\right) + O\left(N \times (|\Omega_i| \times N + |\Xi|\right)$
   - Using BRLES for the update, the complexity is $O(\text{Iter}_{\max} \times M \times O_{\text{BRLES}})$, where $O_{\text{BRLES}} = O((|\Omega_i| + 1)^N \times |\Xi|^N)$.

E. ANALYSIS AND INSIGHTS

This subsection provides a detailed examination of the computational complexities associated with the BR-SSO and BRLES strategies, as well as the implications of these complexities for the operational feasibility of the Sequential Play algorithm.

- **BR-SSO Dependency:** When choosing BR-SSO for the strategy update, the complexity scales polynomial with $\text{Iter}_{\max}$, M, N, $|\Omega_i|$, and $|\Xi|$. This denotes a feasible computational growth, potentially fitting for larger systems.
- **BRLES Dependency:** Choosing BRLES showcases an exponential complexity growth concerning N and possibly M. This makes the Sequential Play algorithm much more computationally demanding with BRLES, especially as N or M rise.
- **Operational Insight:** The algorithm primarily aims for convergence via sequentially updating players' strategies. However, the selection between BR-SSO and BRLES can greatly influence its operational feasibility in real-time systems. System designers should weigh the trade-offs between optimality (with BRLES) and computational efficiency (with BR-SSO) based on their application and the computational resources at their disposal.

VI. NUMERICAL RESULTS

In this section, we assess the system's performance through simulation studies.

Our simulated environment consists of 5 UAVs and a total of 50 MUEs. To simplify the representation and focus on the core aspects of our research, each UAV is paired with a set of 10 MUEs, thereby forming a distinct UAV cell. It's pertinent to note that this association between MUEs and UAVs is predefined for the purpose of this simulation and does not reflect a limitation of the proposed system.

The MUEs are considered static and are spread randomly across a square area measuring $100 \times 100\text{M}^2$. Similarly, while UAVs operate at a predetermined altitude, their horizontal positioning follows a random distribution within the same square region, as depicted in Fig. 2. Blockages, which can impact the communication, are modeled as described in section II-B.

For the reader's sake, the main system parameters are summarized in Table 1.

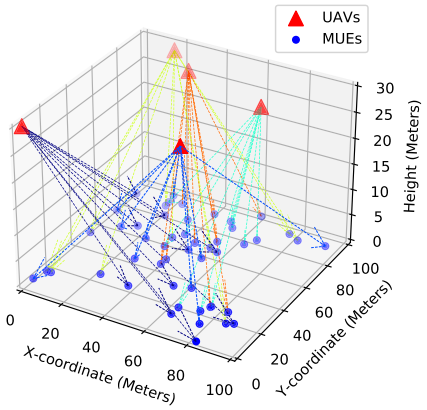

FIGURE 2. Simulation Network in a one-shot game (blockages are omitted).

TABLE 1. Basic simulation settings.

Parameter	Value
Number of UAVs	5
Number of total MUEs	50
Number of users per UAV cell	10
Area Radius	100 m
Fly height	30 m
QoS rate requirement	1 Mbps
Pass loss exponent	2.1
Power level factor	0.15
Noise power spectrum density	-274 dBm/Hz
Carrier Frequency	60 GHz
Subcarrier bandwidth	20 KHz
Number of subcarriers	32
UAVs and MUEs antenna gain	0 dB
Blockage factor	60
Maximum transmit power at the UAV	53 dBm
SNR gap	0 dB

A. CONVERGENCE AND OPTIMALITY

We demonstrate the convergence of the proposed constrained potential game under two scenarios, the BR-SSO dynamics and the best response dynamics via a one-shot simulation (see Fig. 2). The convergence curve of the proposed constrained potential function is shown in Fig. 6. One iteration indicates the algorithm 2 finishes one loop where each UAV player played for one time. It can be observed from the figure that the potential function satisfies the mono-increasing property with each iteration. The value of the potential function under best response dynamics has greater increase changes compared to the BBR-SSO dynamics within each iteration, and the potential function converges at iteration 24 with a higher value than the corresponding BBR-SSO dynamics, which converges at iterations 38 with a lower function value. This is coherent with the dynamics properties, wherein the best dynamics, the best response is achieved by an exhaustive

search of the state space, resulting in a bigger increase in the utility value, thus leading to the same bigger increase in the potential function value. The BR-SSO dynamics are different in that each player only selects a better response within iteration according to algorithm 1, thus leading to less increase amount.

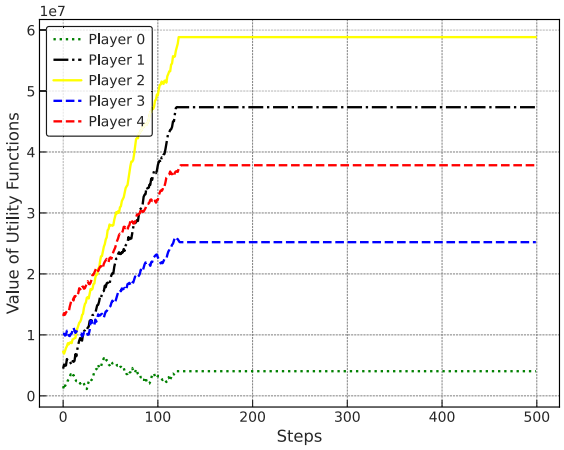

FIGURE 3. Convergence of separate player's utility function under the BRLES dynamics.

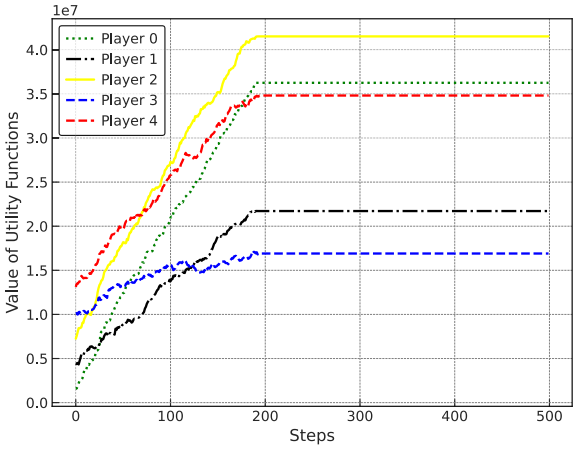

FIGURE 4. Convergence of separate player's utility function under the BR-SSO dynamics.

The convergence graph of each UAV player's utility function under best response dynamics based on local exhaustive search (BRLES) and BR-SSO dynamics is illustrated in the Fig. 3 and Fig. 4, respectively. Each step in the graphs represent a utility value change caused by each play of its own or the other players, that is, the UAV player 0 played at step 0, so the value of the utility function of player 0 is increasing, while in steps 1 to 4, it does not play and the value is increasing or decreasing, depending on the other players' plays. Note the other player's actions can lead to the decrease or increase in UAV player 0 because all players play in their own interests. Note the fluctuations of UAV player 0 do not affect the convergence of the algorithm, although the fluctuations may slow down the convergence of it. Also, we can notice that the increased amount of all UAV players in one iteration is equal to the potential function value increase in the Fig. 6 which is consistent with the theoretical analysis. We also plot the system sum

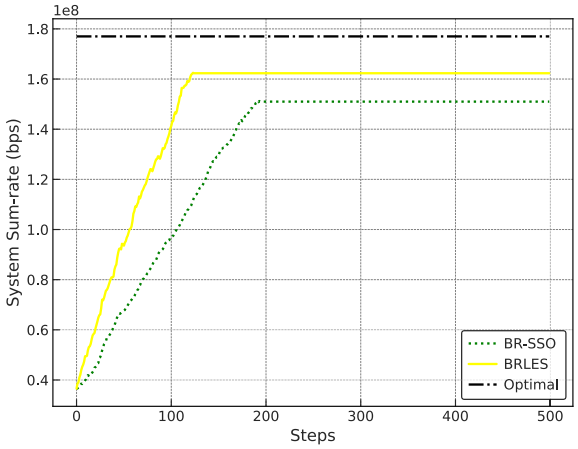

FIGURE 5. Convergence of system sum rate under different algorithm settings.

rate under different algorithm settings, as shown in Fig. 5. The convergence curves of BR-SSO, the best response local exhaustive search (BRLES), and the globally optimal solution are presented for comparison. The results were obtained using a single simulation trial to capture the convergence behavior. The globally optimal solution is plotted by an exhaustive search to evaluate the optimality of our proposed algorithm. It can be seen both BBR-SSO and the BERLES result in local optimum, approximately 162Mbps and 151Mbps, respectively, whereas the global optimum point could only be found through the global exhaustive search method, which is approximately 175Mbps, approximately.

Moreover, as shown in Fig. 5, the network sum rate of the two algorithms is updated in each iteration, and both significantly improve at the convergence time. Furthermore, our proposed BR-SSO algorithm converges slower than the BRLES algorithm, which coincides with the results in Fig. 6, because the better response dynamics do not need to find the optimal solution at each play, and hence has lower complexity.

B. IMPACT OF DIFFERENT BLOCKAGE FACTOR PARAMETER

In this subsection, we illustrate the effect of blockage factor parameter $\mathcal{D}_{i,k}$ on the performance of the system. First, we plot the system sum rate of BR-SSO and BRLES under different blockage factor settings. It can be seen from the Fig. 7, the greater the blockage factor amount, the higher the system sum rate. When $\mathcal{D}_{i,k} = 1$, the system has the lowest sum rate under all dynamics responses. This is because the interference from neighboring UAV cells is significant, causing a large degradation of the sum rate within one UAV cell. This shows that the mmWave UAV cooperative system is not suitable for dense deployment in

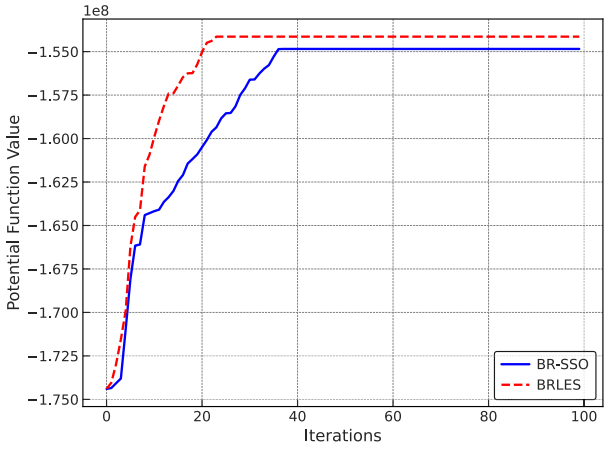

FIGURE 6. Convergence of potential function.

our network model. Note such result is not contradictive to other literature, such as [9], [33], and [34], where the cell area is not crossing with each other. With the increase of decay rate β_{block}, the blockage factor increased accordingly, which indicates the blockage effect becomes more obvious, as can be seen from the Fig. 7, the system sum-rate increased rapidly within the first a few increased amount of blockage factor. When the number reached approximately 160, the system nearly reached the maximum sum-rate point. Subsequently, the increasing trend becomes slower, and it converges after the blockage factor reaches approximately 200, where the system sum rate no longer increases anymore. This phenomenon shows that the blockages play a positive role in the system performance because the interference from nearby UAVs is almost completely blocked. The whole cooperative multi-UAV system was reduced to an independent multi-UAV system. Subsequently, the optimization problem becomes convex where only one optimal point exists.

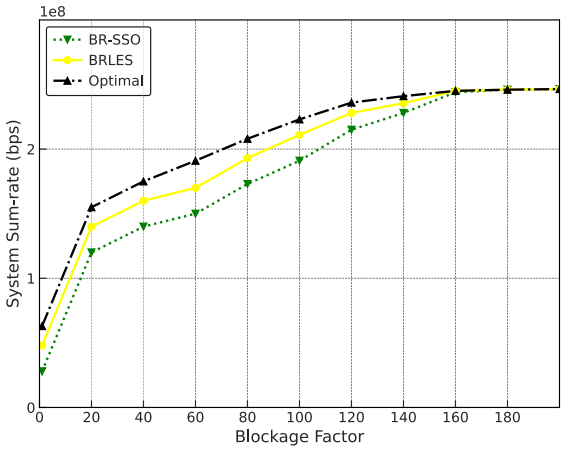

FIGURE 7. System sum rate under different blockage factor settings.

To shed light on why the system sum rate converges after the blockage factor reaches a certain threshold, we also draw the sum-rate and noise power relation graph in Fig. 8 and Fig. 9. It can be seen that the sum rate under BR-SSO dynamics as well as the BRLES dynamics all increase with a decrease in the noise power spectral density (PSD). In BR-SSO dynamics, with a decrease in noise PSD from −224dBm/Hz to −274dBm/Hz, the system sum rate increased from approximately 221Mbps to 252Mbps, approximately. Similarly, as illustrated in the Fig. 8, the system sum rate also increased from approximately 226Mbps to 266Mbps, approximately, as the noise PSD decreased from −224dBm/Hz to −274dBm/Hz. In both figures, when the noise PSD reached approximately -124dBm/Hz, the system reached the noise-limited regime, that is, the system sum rate do not changes with the change in the blockage factor. This is because when the noise PSD is dominant, the total interference suffered by one UAV is negligible compared to the total noise it receives, thus the system exhibits a very lower performance, although it is invariant to the interference it receives.

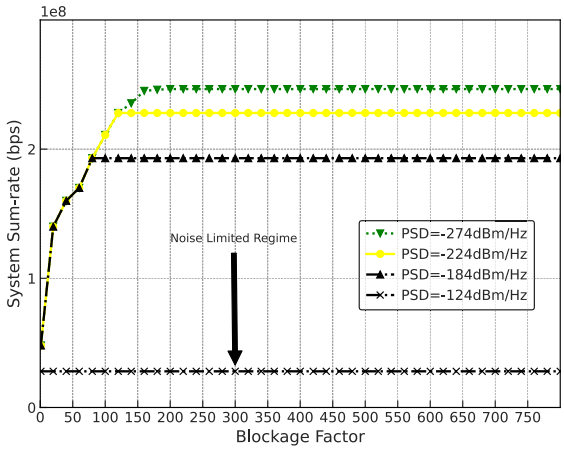

FIGURE 8. System sum rate under BRLES.

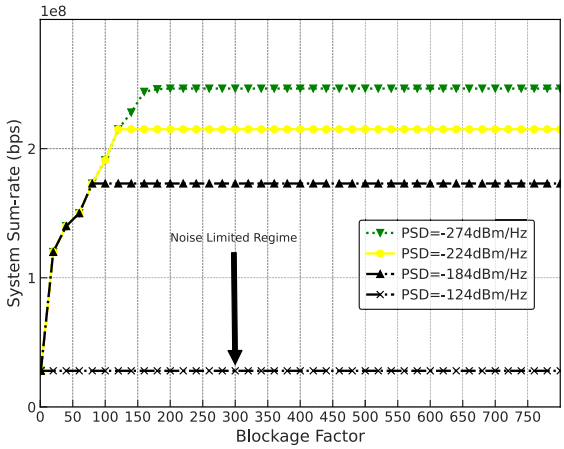

FIGURE 9. System sum rate under BR-SSO.

C. IMPACT OF DIFFERENT POWER LEVELS

We evaluated the performance of our proposed algorithm in terms of different power levels, and similar to [7] and [35] the

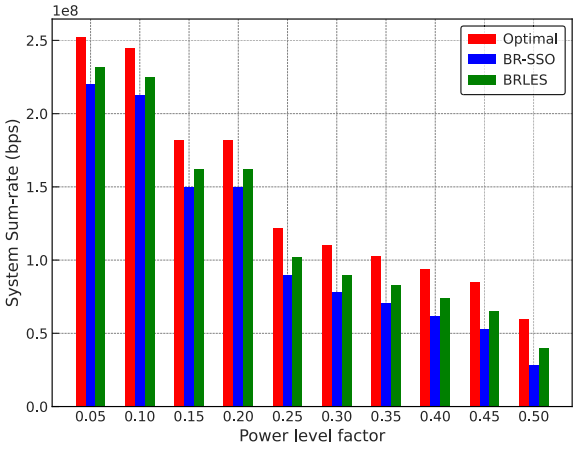

FIGURE 10. System sum rate under different power level factors.

power level factor are set to $\{i/20, i = 1, \cdots, 10\}$. As shown in Fig. 10, with the decrease of power levels, that is, from the power levels 20 to 2, which corresponds to the power level factor 0.05 and 0.5, respectively, the system sum rate decrease too, under all cases, from approximately 220Mbps to 25Mbps in BR-SSO dynamics. Under the optimal and BRLES situations, the sum rate also decreased from 261Mpbs and 225Mbps to nearly 70Mbps and 40Mbps, respectively.

This demonstrates that with more power levels, the discrete assignment is more similar to the continuous power assignment counterpart, showing a greater system performance. In addition, when the power level reaches nearly 18, the performance gain slowes down and became nearly stable, which shows a convergence trend. The worst system performance is under the power level 2, because two power assignment state are feasible, which cause a very likely state to be far from optimal.

D. IMPACT OF QOS RATE REQUIREMENT

In this subsection, we evaluate the sum rate of UAV 1 under a QoS requirement rate 1Mbps. To simplify, we assume that the QoS requirement rates of all MUEs are equal. As shown in the Fig. 11, the rate of the non-QoS case significantly surpasses that of all the other cases for almost all MUEs, with six MUEs nearly reaching their maximum rate. This shows that their SINRs are dominant compared with the other MUEs. It can find that this result is owing to the non-QoS property that the rate is allocated to the MUE that has the most channel conditions, whereas the MUE that has the worst channel condition is allocated the least amount of rate. In the BR-SSO situation, the performance gap is not as obvious as in the non-QoS case, but the MUE 8 and 9 still have the greatest rate allocation, the MUE 2, has less rate allocation compared to the non-QoS case, but the performance gap is not as significant compare to the MUE 0 as in the non-QoS case. This is because although MUE 0 has the worst channel condition, we still should allocate the minimum rate to it to satisfy its QoS rate requirement, causing a relatively lower rate difference. In the BRLES situation, the same phenomenon occurs, although it can also be seen that nearly the rate allocated to all MUEs is greater than that in BR-SSO case, with only a few exceptions.

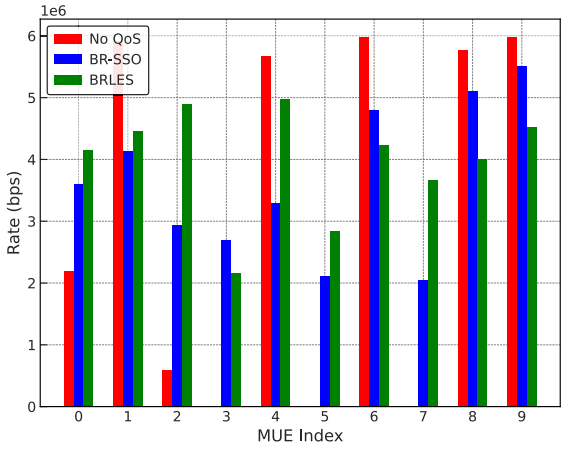

FIGURE 11. MUE rate comparison within one UAV.

The overall Jain fairness index of the system with respect to different QoS rate requirement is evaluated in Fig. 12. It can be seen that the system fairness improves with an increase in the QoS rate requirement. All three cases, that is, optimal, BR-SSO, and BRLES have the lowest system fairness index when the QoS rate requirement is zero.

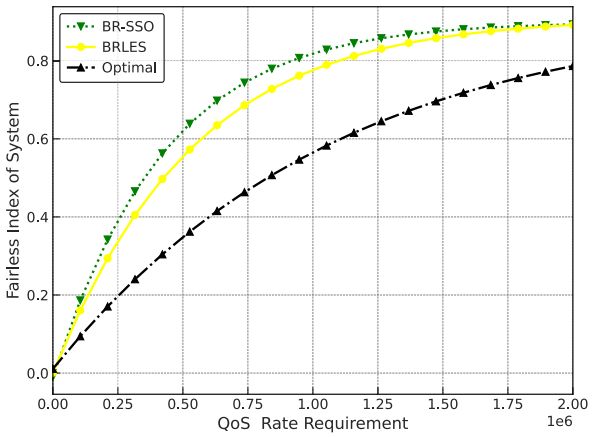

FIGURE 12. Impact of different QoS rate requirements on system fairness index.

VII. CONCLUSION AND FUTURE WORK

In this paper, we introduced a novel resource allocation scheme for multi-UAV millimeter-wave cooperative OFDMA networks to address the challenge of heterogeneous user data rate QoS requirements. Our formulated nonconvex and NP-hard joint optimization problem was transformed into the Subcarrier and Power Resource Efficient Cooperative Potential Game (SRECPG).

Critically, our introduced BR-SSO algorithm based on better response dynamics significantly reduces computational

efforts compared to exhaustive search best response dynamics, and still ensures convergence to a NE. Specifically, the results highlight that our BR-SSO approach converges in fewer iterations and achieves a sum rate closer to that of the optimal methods with less computational overhead. Additionally, with varied QoS rate requirements, the fairness of our system improved notably, emphasizing the adaptability of our approach.

Through extensive simulations, we underscore the effectiveness of the proposed SRECPG and BR-SSO algorithms. The obtained results showcase marked improvements in throughput, fairness, and QoS guarantees compared with the baseline schemes.

In this study, we did not consider imperfect CSI due to estimation errors and finite data feedback. This is a limitation of our study, as the CSI is not usually perfectly perceived in practice because of the air links between UAVs and ground users. In a future study, we plan to address this limitation by considering the following directions:

- CSI acquisition: We will develop new methods for acquiring CSI in UAV networks, considering the challenges of air links and finite data feedback.
- Robust optimization: We plan to develop robust optimization frameworks for UAV networks that can tolerate CSI error.
- Other UAV networks: We will extend our work to support other types of UAV networks, such as heterogeneous UAV networks and UAV networks with dynamic topologies.

REFERENCES

[1] P. Li and J. Xu, "Fundamental rate limits of UAV-enabled multiple access channel with trajectory optimization," *IEEE Trans. Wireless Commun.*, vol. 19, no. 1, pp. 458–474, Jan. 2020.

[2] D. Tyrovolas, P.-V. Mekikis, S. A. Tegos, P. D. Diamantoulakis, C. K. Liaskos, and G. K. Karagiannidis, "Energy-aware design of UAV-mounted RIS networks for IoT data collection," *IEEE Trans. Commun.*, vol. 71, no. 2, pp. 1168–1178, Feb. 2023.

[3] Z. Han, Z. Ji, and K. J. R. Liu, "Non-cooperative resource competition game by virtual referee in multi-cell OFDMA networks," *IEEE J. Sel. Areas Commun.*, vol. 25, no. 6, pp. 1079–1090, Aug. 2007.

[4] B. Ahuja, D. Mishra, and R. Bose, "Fair subcarrier allocation for securing OFDMA in IoT against full-duplex hybrid attacker," *IEEE Trans. Inf. Forensics Security*, vol. 16, pp. 2898–2911, 2021.

[5] P. X. Nguyen, D.-H. Tran, O. Onireti, P. T. Tin, S. Q. Nguyen, S. Chatzinotas, and H. V. Poor, "Backscatter-assisted data offloading in OFDMA-based wireless-powered mobile edge computing for IoT networks," *IEEE Internet Things J.*, vol. 8, no. 11, pp. 9233–9243, Jun. 2021.

[6] K. Xie, J. Cao, X. Wang, and J. Wen, "Optimal resource allocation for reliable and energy efficient cooperative communications," *IEEE Trans. Wireless Commun.*, vol. 12, no. 10, pp. 4994–5007, Oct. 2013.

[7] H. Zhang, L. Venturino, N. Prasad, P. Li, S. Rangarajan, and X. Wang, "Weighted sum-rate maximization in multi-cell networks via coordinated scheduling and discrete power control," *IEEE J. Sel. Areas Commun.*, vol. 29, no. 6, pp. 1214–1224, Jun. 2011.

[8] E. Bjornson, N. Jalden, M. Bengtsson, and B. Ottersten, "Optimality properties, distributed strategies, and measurement-based evaluation of coordinated multicell OFDMA transmission," *IEEE Trans. Signal Process.*, vol. 59, no. 12, pp. 6086–6101, Dec. 2011.

[9] Q. D. La, Y. H. Chew, and B. H. Soong, "Performance analysis of downlink multi-cell OFDMA systems based on potential game," *IEEE Trans. Wireless Commun.*, vol. 11, no. 9, pp. 3358–3367, Sep. 2012.

[10] W. Yu, T. Kwon, and C. Shin, "Multicell coordination via joint scheduling, beamforming, and power spectrum adaptation," *IEEE Trans. Wireless Commun.*, vol. 12, no. 7, pp. 3300–3313, Jul. 2013.

[11] J.-S. Pang, G. Scutari, F. Facchinei, and C. Wang, "Distributed power allocation with rate constraints in Gaussian parallel interference channels," *IEEE Trans. Inf. Theory*, vol. 54, no. 8, pp. 3471–3489, Aug. 2008.

[12] S. Lahoud, K. Khawam, S. Martin, G. Feng, Z. Liang, and J. Nasreddine, "Energy-efficient joint scheduling and power control in multi-cell wireless networks," *IEEE J. Sel. Areas Commun.*, vol. 34, no. 12, pp. 3409–3426, Dec. 2016.

[13] J. Zheng, Y. Wu, N. Zhang, H. Zhou, Y. Cai, and X. Shen, "Optimal power control in ultra-dense small cell networks: A game-theoretic approach," *IEEE Trans. Wireless Commun.*, vol. 16, no. 7, pp. 4139–4150, Jul. 2017.

[14] W. Yu, G. Ginis, and J. M. Cioffi, "Distributed multiuser power control for digital subscriber lines," *IEEE J. Sel. Areas Commun.*, vol. 20, no. 5, pp. 1105–1115, Jun. 2002.

[15] N. Ksairi, P. Bianchi, P. Ciblat, and W. Hachem, "Resource allocation for downlink cellular OFDMA systems—Part II: Practical algorithms and optimal reuse factor," *IEEE Trans. Signal Process.*, vol. 58, no. 2, pp. 735–749, Feb. 2010.

[16] F. Wang, M. Krunz, and S. Cui, "Price-based spectrum management in cognitive radio networks," *IEEE J. Sel. Topics Signal Process.*, vol. 2, no. 1, pp. 74–87, Feb. 2008.

[17] C.-K. Chau, "A game-theoretical study of robust networked systems," *IEEE J. Sel. Areas Commun.*, vol. 26, no. 7, pp. 1250–1259, Sep. 2008.

[18] L. Liang and G. Feng, "A game-theoretic framework for interference coordination in OFDMA relay networks," *IEEE Trans. Veh. Technol.*, vol. 61, no. 1, pp. 321–332, Jan. 2012.

[19] F. Wang, W. Chen, H. Tang, and Q. Wu, "Joint optimization of user association, subchannel allocation, and power allocation in multi-cell multi-association OFDMA heterogeneous networks,' *IEEE Trans. Commun.*, vol. 65, no. 6, pp. 2672–2684, Jun. 2017, doi: 10.1109/TCOMM.2017.2678986.

[20] S. Buzzi, G. Colavolpe, D. Saturnino, and A. Zappone, "Potential games for energy-efficient power control and subcarrier allocation in uplink multicell OFDMA systems," *IEEE J. Sel. Topics Signal Process.*, vol. 6, no. 2, pp. 89–103, Apr. 2012.

[21] C. W. Tan, M. Chiang, and R. Srikant, "Maximizing sum rate and minimizing MSE on multiuser downlink: Optimality, fast algorithms and equivalence via max-min SINR," *IEEE Trans. Signal Process.*, vol. 59, no. 12, pp. 6127–6143, Dec. 2011.

[22] L. Zheng, D. W. H. Cai, and C. W. Tan, "Max-min fairness rate control in wireless networks: Optimality and algorithms by perron-frobenius theory," *IEEE Trans. Mobile Comput.*, vol. 17, no. 1, pp. 127–140, Jan. 2018.

[23] N. Zhang, S. Zhang, J. Zheng, X. Fang, J. W. Mark, and X. Shen, "QoE driven decentralized spectrum sharing in 5G networks: Potential game approach," *IEEE Trans. Veh. Technol.*, vol. 66, no. 9, pp. 7797–7808, Sep. 2017.

[24] D. W. K. Ng and R. Schober, "Resource allocation and scheduling in multi-cell OFDMA systems with decode-and-forward relaying," *IEEE Trans. Wireless Commun.*, vol. 10, no. 7, pp. 2246–2258, Jul. 2011.

[25] Q. D. La, Y. H. Chew, and B. H. Soong, "An interference-minimization potential game for OFDMA-based distributed spectrum sharing systems," *IEEE Trans. Veh. Technol.*, vol. 60, no. 7, pp. 3374–3385, Sep. 2011.

[26] M. Tao, Y.-C. Liang, and F. Zhang, "Adaptive resource allocation for delay differentiated traffic in multiuser OFDM systems," in *Proc. IEEE Int. Conf. Commun.*, vol. 10, Jun. 2006, pp. 4403–4408.

[27] A. Leshem, E. Zehavi, and I. T. Mar, "Game theory and the frequency selective interference channel," *IEEE Signal Process. Mag.*, vol. 26, no. 5, pp. 28–40, Sep. 2009.

[28] S. Li, Z. Shao, and J. Huang, "ARM: Anonymous rating mechanism for discrete power control," *IEEE Trans. Mobile Comput.*, vol. 16, no. 2, pp. 326–340, Feb. 2017.

[29] Y.-F. Liu and Y.-H. Dai, "On the complexity of joint subcarrier and power allocation for multi-user OFDMA systems," *IEEE Trans. Signal Process.*, vol. 62, no. 3, pp. 583–596, Feb. 2014, doi: 10.1109/TSP.2013.2293130.

[30] S. Rose, S. Perlaza, S. Lasaulce, and S. Debbah, "Learning equilibria with partial information in wireless networks," in *Proc. IEEE Commun. Mag. Special Issue Game Theory Wireless Commun.*, Aug. 2011, pp. 136–142.

[31] A. Gjendemsjo, D. Gesbert, G. E. Oien, and S. G. Kiani, "Binary power control for sum rate maximization over multiple interfering links," *IEEE Trans. Wireless Commun.*, vol. 7, no. 8, pp. 3164–3173, Aug. 2008.

[32] G. Scutari, F. Facchinei, P. Song, D. P. Palomar, and J.-S. Pang, "Decomposition by partial linearization: Parallel optimization of multi-agent systems," *IEEE Trans. Signal Process.*, vol. 62, no. 3, pp. 641–656, Feb. 2014.
[33] S.-Y. Kim, J.-A. Kwon, and J.-W. Lee, "Sum-rate maximization for multicell OFDMA systems," *IEEE Trans. Veh. Technol.*, vol. 64, no. 9, pp. 4158–4169, Sep. 2015, doi: 10.1109/TVT.2014.2363476.
[34] H. Yang and X. Xie, "Energy-efficient joint scheduling and resource management for UAV-enabled multicell networks," *IEEE Syst. J.*, vol. 14, no. 1, pp. 363–374, Mar. 2020.
[35] J. Zheng, Y. Cai, Y. Liu, Y. Xu, B. Duan, and X. Shen, "Optimal power allocation and user scheduling in multicell networks: Base station cooperation using a game-theoretic approach," *IEEE Trans. Wireless Commun.*, vol. 13, no. 12, pp. 6928–6942, Dec. 2014.
[36] A. F. Isnawati, "A survey of game theoretical approach in cognitive radio network and 5G-6G communications," *J. Commun.*, vol. 17, no. 10, pp. 830–843, Oct. 2022, doi: 10.12720/JCM.17.10.830-843.
[37] A. F. Isnawati and M. A. Afandi, "Performance analysis of game theoretical approach for power control system in heterogeneous network," *Int. J. Intell. Eng. Syst.*, vol. 15, no. 3, pp. 397–405, 2022, doi: 10.22266/IJIES2022.0630.33.
[38] P. S. Bithas, V. Nikolaidis, A. G. Kanatas, and G. K. Karagiannidis, "UAV-to-ground communications: Channel modeling and UAV selection," *IEEE Trans. Commun.*, vol. 68, no. 8, pp. 5135–5144, Aug. 2020.
[39] J. Li, Y. Niu, H. Wu, B. Ai, R. He, N. Wang, and S. Chen, "Joint optimization of relay selection and transmission scheduling for UAV-aided mmWave vehicular networks," *IEEE Trans. Veh. Technol.*, vol. 72, no. 5, pp. 6322–6334, May 2023.
[40] Y. Liu, K. Xiong, Y. Lu, Q. Ni, P. Fan, and K. B. Letaief, "UAV-aided wireless power transfer and data collection in Rician fading," *IEEE J. Sel. Areas Commun.*, vol. 39, no. 10, pp. 3097–3113, Oct. 2021.
[41] W. Feng, J. Wang, Y. Chen, X. Wang, N. Ge, and J. Lu, "UAV-aided MIMO communications for 5G Internet of Things," *IEEE Internet Things J.*, vol. 6, no. 2, pp. 1731–1740, Apr. 2019.

TONG WANG (Member, IEEE) received the M.S. degree in computer software from Nankai University and the Ph.D. degree in computer architecture from Wuhan University. He is currently an Associate Professor with the Department of Computer Science, School of Information Engineering, Hubei University of Economics, China. He was a Visiting Scholar with the Department of Computer Science, College of Engineering and Applied Sciences, Western Michigan University, MI, USA. His current research interests include intelligent reflecting surfaces, energy-efficient wireless communications, mobile edge computing, wireless power transfer, and unmanned aerial vehicle communications. He is a member of the Chinese Computer Federation.

CHUANCHUAN YOU (Member, IEEE) received the M.E. degree in software engineering with a focus on software development in the field of financial services from Peking University and the B.Eng. degree in computer software with a focus on software application from the Wuhan University of Science and Technology, China, in 2000 and 2005, respectively. He is currently pursuing the Ph.D. degree with the School of Computer Science, Wuhan University, Wuhan, China. He is also a Lecturer with the School of Information Engineering, Hubei University of Economics, Wuhan. He has been a Visiting Scholar with the International Institute of Next Generation Internet, Macau University of Science and Technology, Macau, since 2022. His research interests include artificial intelligence, block chain, big data analysis, robotics, and social computing. He has successively served as a member for the China Computer Society, the Vice Chairperson for Wuhan Academic Committee of CCF YOCSEF (2012–2014), and an AC Member for CCF YOCSEF Wuhan, from 2011 to 2014.

ZHOU HE received the Ph.D. degree in electronic science and technology from the Huazhong University of Science and Technology. She is currently with the School of Information Engineering, Hubei University of Economics, Wuhan, China, where she is also an Associate Professor. Her research interests include the area of 5G/6G mobile communication technology, advanced modulation technology of optical communication networks, and AI technology. As the first author, she has published more than 20 papers. In the past five years, she has presided over or participated in seven provincial and bureau level projects.

YOUTIAN WANG received the Bachelor of Business degree from Peking University, in 1998, the Master of Management degree from Tsinghua University, in 2007, and the Ph.D. degree in management from the Huazhong University of Science Technology, in 2014. He is currently an Associate Professor in information systems with the Hubei University of Economics. He has published some treatises about information systems and computer simulations and presided some information system design and development project for some organizations. He is also actively developing NilNul information systems, which open sourced at github, represents knowledge for different domains in code, and can help them to learn and deploy such knowledge in education and business easier and more efficient.